Characterization of Surrounding Greenery and Housing Prices Using Street View Images Across Urban Local Climate Zones and Cities of Metro Manila

Jeremiah L. Marimon[1], Karl Adrian P. Vergara[1]

[1]Department of Geodetic Engineering, University of the Philippines, Diliman, Quezon City, Philippines – (marimon1635@gmail.com, kpvergara@up.edu.ph)

Keywords: Green View Index, Hedonic Pricing Model, Local Climate Zones, Urban Greenery, Metro Manila.

Abstract

Urban greenery is increasingly recognized as a factor that can influence residential property values. Despite this, few studies have explored this relationship using street-level perspectives or across diverse urban forms in developing megacities like Metro Manila. This study examines the relationship between visible greenery and housing prices in Metro Manila, utilizing Google Street View images sampled at 100-meter intervals and processed through a PSPNet-based semantic segmentation model pretrained on the ADE20K dataset to calculate the Green View Index (GVI). GVI values were averaged within 400-meter radius buffers around 1007 housing units sourced from Lamudi, with an 80-20 train-test split. Spatial autocorrelation analyses (Getis-Ord Gi* and Local Moran's I) identified heterogeneous clusters of greenery and housing prices across the region. Hedonic pricing models, incorporating structural/housing attributes, location, proximity to amenities, facility density, and GVI, were estimated at three scales: the entire Metro Manila area, eight urban Local Climate Zones (LCZs), and individual cities. In the overall Metro Manila model, GVI exhibited a positive association with housing prices, suggesting that higher visible greenery generally enhances property values. However, this effect varied across LCZ-based and city-based analyses: GVI significantly increased prices in open mid-rise (LCZ 5) and open low-rise (LCZ 6) areas, as well as in urbanized centers like Makati and Manila, while showing negligible impact in compact and mixed-built zones. These findings underscore the value of context-specific urban greening to boost property values and inform sustainable planning in Metro Manila.

1. Introduction

Urban greenery—trees, shrubs, parks, and other vegetation visible at street level—plays a critical role in urban livability. It mitigates air pollution, reduces noise, improves thermal comfort, and enhances the pedestrian experience and streetscape aesthetics (Qian et al., 2015; Dimoudi and Nikolopoulou, 2003). Beyond ecological benefits, visible greenery contributes to quality of life and can increase property values, as housing markets often capitalize on the environmental, recreational, and perceived safety benefits associated with green surroundings (Zhang and Dong, 2018). However, traditional remote sensing indicators, such as the Normalized Difference Vegetation Index (NDVI), quantify canopy cover from above and do not capture the human visual experience at street level—an aspect that is often most relevant to daily life and housing choices (Yang et al., 2009).

The Green View Index (GVI) was developed to address this gap by measuring the proportion of vegetation pixels in street imagery, thereby capturing greenery as perceived by pedestrians (Li et al., 2015). Recent developments in computer vision including semantic segmentation models such as Pyramid Scene Parsing Network (PSPNet), have enabled accurate, large-scale extraction of vegetation pixels from street images (Stubbings et al., 2019; Zhao et al., 2017). These advances make automated GVI computation feasible for metropolitan-scale applications. By leveraging such techniques, human-scale greenery metrics can be integrated with housing-market data to estimate more precisely the implicit value of street-level greenery across heterogeneous urban environments.

Residential housing prices are influenced by intrinsic attributes (e.g., floor area, number of bedrooms) and extrinsic factors (e.g., proximity to employment centers, amenities, and the quality of the surrounding environment) (Wittowsky et al., 2020). Hedonic pricing models, which decompose prices into contributions from these attributes, remain the standard approach to estimate the monetary contribution of these factors. Importantly, the marginal value of visible greenery is likely context-dependent: a given increase or decrease in GVI may be valued differently in compact high-density areas compared with open low-density neighborhoods. To capture this heterogeneity, the Local Climate Zone (LCZ) framework was employed, which classifies urban areas by building density, height, and surface cover (Stewart and Oke, 2012). Using LCZs enables context-specific analysis and helps isolate the effect of street-level greenery across compact, open, or mixed urban forms.

Despite rapid urbanization in Metro Manila, few studies have quantified street-level greenery at scale, with prior studies relying on overhead remote sensing. The relationship between street-level greenery and housing prices, particularly across LCZ classes and administrative boundaries in the region, remains underexplored. This study addresses that gap by integrating GVI derived from Google Street View images with residential property data across Metro Manila. Automated semantic segmentation, spatial analysis, and hedonic price modelling are integrated to assess how visible greenery is distributed in the metropolitan area and how it affects housing values.

Specifically, the study aims to: (1) quantify and visualize the spatial distribution of greenery using GVI derived from street-level imagery; (2) examine the spatial patterns of housing prices; and (3) develop hedonic pricing models to assess GVI's impact alongside structural/housing, location, proximity, and density factors at region-wide, LCZ-specific, and city-level scales. The findings can guide policymakers in zoning, green space allocation, and the development of sustainable urban strategies that balance ecological and economic benefits.

2. Review of Related Literature

2.1 Local Climate Zones

The Local Climate Zones (LCZ) classification scheme is a system developed by Stewart and Oke (2012) to categorize urban and suburban areas based on their distinct climatic and thermal characteristics. It classifies different microenvironments by surface cover, building form, materials, and human activity, and ranges from dense urban areas with high-rise buildings to open spaces like parks and water bodies. There are 17 local climate zones as described in Figure 1, with 1-10 considered as "urban or built" types and A-G considered as "land cover" types.

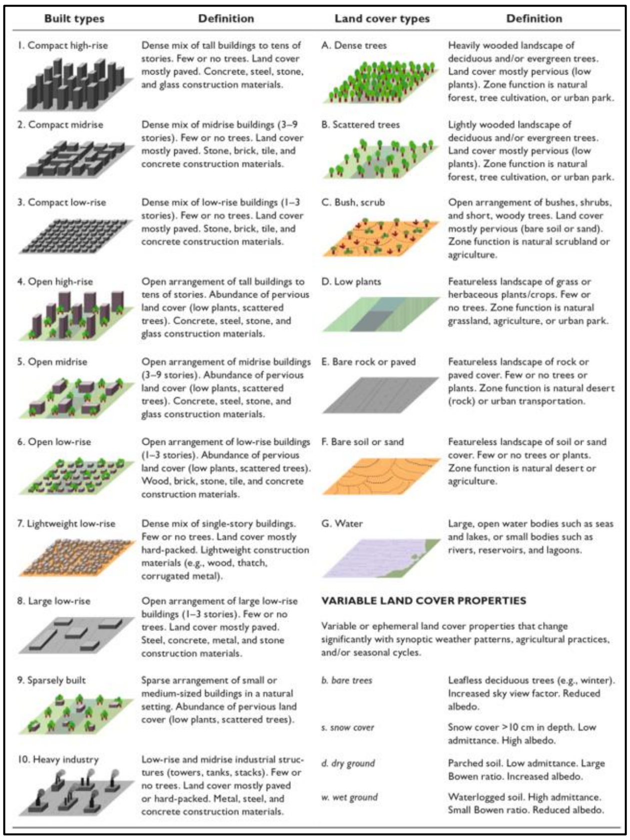

Built types	Definition	Land cover types	Definition
1. Compact high-rise	Dense mix of tall buildings to tens of stories. Few or no trees. Land cover mostly paved. Concrete, steel, stone, and glass construction materials.	A. Dense trees	Heavily wooded landscape of deciduous and/or evergreen trees. Land cover mostly pervious (low plants). Zone function is natural forest, tree cultivation, or urban park.
2. Compact midrise	Dense mix of midrise buildings (3–9 stories). Few or no trees. Land cover mostly paved. Stone, brick, tile, and concrete construction materials.	B. Scattered trees	Lightly wooded landscape of deciduous and/or evergreen trees. Land cover mostly pervious (low plants). Zone function is natural forest, tree cultivation, or urban park.
3. Compact low-rise	Dense mix of low-rise buildings (1–3 stories). Few or no trees. Land cover mostly paved. Stone, brick, tile, and concrete construction materials.	C. Bush, scrub	Open arrangement of bushes, shrubs, and short, woody trees. Land cover mostly pervious (bare soil or sand). Zone function is natural scrubland or agriculture.
4. Open high-rise	Open arrangement of tall buildings to tens of stories. Abundance of pervious land cover (low plants, scattered trees). Concrete, steel, stone, and glass construction materials.	D. Low plants	Featureless landscape of grass or herbaceous plants/crops. Few or no trees. Zone function is natural grassland, agriculture, or urban park.
5. Open midrise	Open arrangement of midrise buildings (3–9 stories). Abundance of pervious land cover (low plants, scattered trees). Concrete, steel, stone, and glass construction materials.	E. Bare rock or paved	Featureless landscape of rock or paved cover. Few or no trees or plants. Zone function is natural desert (rock) or urban transportation.
6. Open low-rise	Open arrangement of low-rise buildings (1–3 stories). Abundance of pervious land cover (low plants, scattered trees). Wood, brick, stone, tile, and concrete construction materials.	F. Bare soil or sand	Featureless landscape of soil or sand cover. Few or no trees or plants. Zone function is natural desert or agriculture.
7. Lightweight low-rise	Dense mix of single-story buildings. Few or no trees. Land cover mostly hard-packed. Lightweight construction materials (e.g., wood, thatch, corrugated metal).	G. Water	Large, open water bodies such as seas and lakes, or small bodies such as rivers, reservoirs, and lagoons.
8. Large low-rise	Open arrangement of large low-rise buildings (1–3 stories). Few or no trees. Land cover mostly paved. Steel, concrete, metal, and stone construction materials.	**VARIABLE LAND COVER PROPERTIES** Variable or ephemeral land cover properties that change significantly with synoptic weather patterns, agricultural practices, and/or seasonal cycles.	
9. Sparsely built	Sparse arrangement of small or medium-sized buildings in a natural setting. Abundance of pervious land cover (low plants, scattered trees).	*b. bare trees*	Leafless deciduous trees (e.g., winter). Increased sky view factor. Reduced albedo.
		s. snow cover	Snow cover >10 cm in depth. Low admittance. High albedo.
10. Heavy industry	Low-rise and midrise industrial structures (towers, tanks, stacks). Few or no trees. Land cover mostly paved or hard-packed. Metal, steel, and concrete construction materials.	*d. dry ground*	Parched soil. Low admittance. Large Bowen ratio. Increased albedo.
		w. wet ground	Waterlogged soil. High admittance. Small Bowen ratio. Reduced albedo.

Figure 1. Urban and natural Local Climate Zone definitions

In this study, only LCZs 1 to 9 were considered as they capture the dominant urban residential morphologies of Metro Manila. The short descriptions of these nine zones are as follows:

- **Compact zones (LCZ 1–3)** describe dense urban areas with little open space or vegetation. LCZ 1 is made up of tall high-rise buildings, LCZ 2 consists of mid-rise buildings packed closely together, and LCZ 3 covers low-rise housing.
- **Open zones (LCZ 4–6)** include buildings with more space between them and greater vegetation cover. LCZ 4 has tall buildings but also more open ground, LCZ 5 includes mid-rise buildings with yards and street trees, while LCZ 6 is dominated by low buildings surrounded by gardens and lawns.
- **Mixed-built forms (LCZ 7–9)** capture special cases. LCZ 7 refers to lightweight low-rise housing often found in informal or temporary areas, LCZ 8 includes large, low industrial or commercial buildings like warehouses or malls, and LCZ 9 is sparsely built, with scattered structures and large areas of open or vegetated ground, often marking the urban–rural transition.

3. Materials and Methods

3.1 Study Area

The research focuses on Metro Manila, officially designated as the National Capital Region (NCR) in the Philippines. It serves as the country's center of government, finance, business, and culture. The region is composed of 17 local government units.

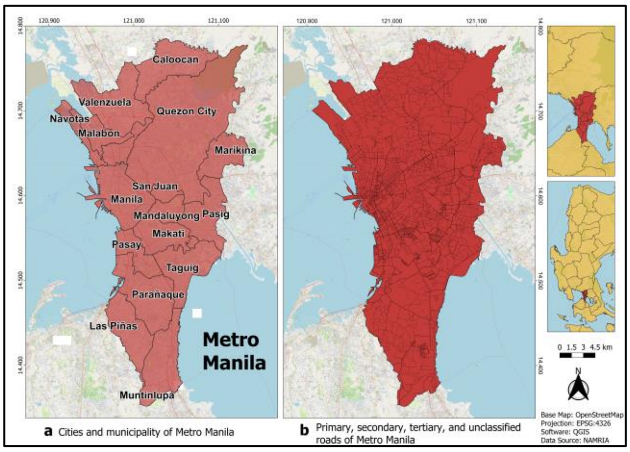

Figure 2. Location and road network of the study area

3.2 Materials

Street-level imagery was obtained from Google Street View using Street View Download 360 Pro software. Images were in JPEG format with dimensions of 1664×832 pixels and included geolocation and timestamp metadata. Housing price data (n=1007 listings after cleaning) were scraped from the Lamudi real estate website in May 2024, January 2025, and March 2025 (Lamudi Philippines, 2024-2025). Local Climate Zone data was sourced from Project AiRMoVE (Ramos et al., 2024), and the Points of Interest (amenities) were obtained from OpenStreetMap (OpenStreetMap contributors, n.d.). QGIS, ArcMap, and Google Colab were used for preprocessing, visualization, and modelling of the datasets, and in conducting the analyses.

3.3 Methods

The methodology comprises three parts: (1) greenery quantification, (2) spatial distribution analyses using Getis-Ord Gi* and Local Moran's I, and (3) hedonic pricing models.

3.3.1 Greenery Quantification: Street-view panoramas were acquired at 100-m intervals across the study area (Wu et al., 2020). To handle computational demands from large-area downloads and processing, the study area was partitioned into six grids and processed sequentially. Vegetation pixels were extracted using a PSPNet-based semantic segmentation model pretrained on the ADE20K dataset (Zhou et al., 2017). The model features a ResNet-50 (dilated) encoder backbone, pyramid pooling module, and a decoder applied with deep supervision, achieving 80.13% accuracy with multiscale testing (CSAILVision, n.d.). From the ADE20K dataset's 150 annotated categories, six categories were considered as greenery: tree, grass, plant, flower, palm, and canopy. For each panorama, the Green View Index (GVI) was calculated as the percentage of greenery pixels over total pixels following equation 1, based on Li et al. (2015).

$$Green\ view = \frac{\sum Area_g}{\sum Area_t} \times 100\% \qquad (1)$$

https://doi.org/10.5194/isprs-archives-XLVIII-5-W4-2025-159-2026 | © Author(s) 2026. CC BY 4.0 License.

where $Area_g$ = number of greenery pixels in panorama
$Area_t$ = total number of pixels in panorama

Residential GVI was calculated as the mean of all the GVI points within a 400-meter buffer around each housing unit. Model accuracy was validated against manual segmentation on 100 random images using Pearson's correlation.

3.3.2 Spatial Distribution Analyses: The study area was tessellated into hexagons of inradius 400 meters each (matching the radius of the residential GVI buffer). Getis-Ord Gi* statistics were computed to identify and map hotspots (high-value clusters) and coldspots (low-value clusters) for both GVI and housing prices. Anselin's Local Moran's I was then applied to detect localized clusters and spatial outliers to reveal the presence of spatial imbalances in both street greenery and property values.

3.3.3 Hedonic Pricing Models: Semi-log (log-linear) hedonic regression models were constructed with the log transformation of price, ln(Price), as the dependent variable and five predictors: Location, Structural/Housing, Proximity, Density, and GVI. The form of the hedonic model is as follows:

$$\ln(P) = \beta_0 + \beta_1 * (Location) + \beta_2 * (Structural/Housing) + \beta_3 * (Proximity) + \beta_4 * (Density) + \beta_5 * (GVI) + \epsilon_i \quad (2)$$

where P = price of the residential unit
β_0 = intercept
β_k = coefficient slope from k = 1 to k = 5
ϵ_i = error term

The first four predictors are composite indices—each a weighted aggregate of standardized sub-variables. Location combines distance to the nearest central business district (CBD) and city center. Structure/Housing aggregates floor area, plot ratio, bathroom count, and bedroom count. Proximity averages distances to eight amenities (bus stop, school, hospital, mall, park, subway, restaurant, tourist site). Density counts the number of those amenities within a 1 km radius. The fifth predictor, residential GVI, is the mean GVI of all points within 400 m of the housing unit.

Distance-related variables were first reciprocated prior to standardization so that shorter distances corresponded to higher scores. The four composite indices were then calculated as weighted averages of the standardized sub-variables, with weights derived from the Analytic Hierarchy Process (AHP) using pairwise comparisons on the Saaty 1–9 scale. Expert judgements were obtained from an urban planner (25 years' experience), a municipal engineer (30 years' experience), and an architect/environmental planner (5 years' experience). Consistency ratios met the recommended threshold of < 0.10 for all experts, except for two comparisons by the municipal engineer (0.124 and 0.104), which remained close to the acceptable limit. Due to time and logistical constraints, only three experts were consulted for the AHP.

Outliers were treated depending on the variable's distribution using one or a combination of: 1.5×IQR filtering, log transformations, Gaussian mixture modelling, and 5% winsorization.

Models were estimated for (a) the entire Metro Manila dataset, (b) individual urban LCZs, and (c) cities, with 80/20 train–test splits. Multicollinearity was checked via Variance Inflation Factors, while model performance was evaluated via coefficients, p-values, and R^2.

4. Results and Discussion

4.1 Distribution of Collected GSV Images

A total of 68286 Google Street View (GSV) panoramas were acquired (47,378 within Metro Manila). Seven major spatial coverage gaps were identified; since these are predominantly located in non-residential or otherwise inaccessible areas (excluding some gated communities), their impact on subsequent housing-price modelling is expected to be minimal.

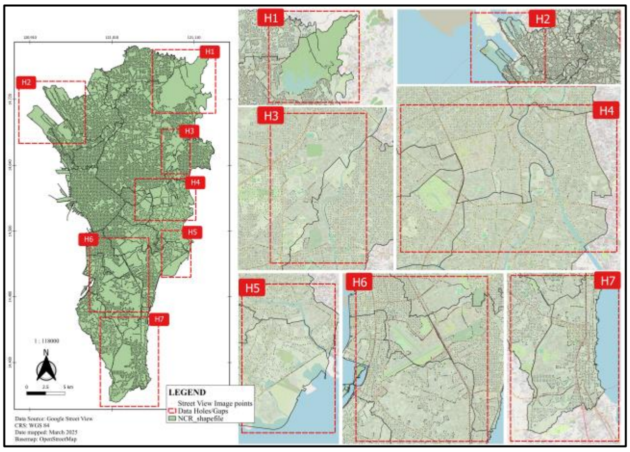

Figure 3. Spatial Data Gaps in the Street View Images Collected

The temporal variability of the street view images ranges from 2013 to 2024, with 85% acquired between 2020 and 2024. Despite this variation, its potential impact on the modelling is likely minimal, given that older street view images are predominantly in areas that experience minimal urban change (Android Police, 2023); street greenery tends to be more stable than other forms of green space (Chen, Zhou, and Li, 2020); and temporal misalignments of up to two years have been used (An et al., 2023).

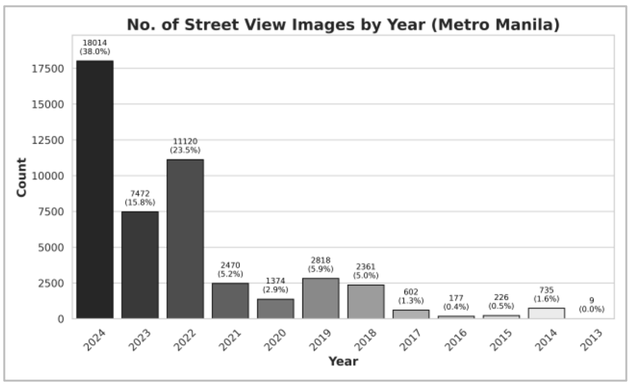

Figure 4. Temporal Gaps in the Collected Street View Images

4.2 Accuracy Assessment

Model GVI correlates strongly with manual segmentation (R^2 = 0.909; Pearson r = 0.953), indicating reliable vegetation extraction. This is very close to the reported values of 0.971 (using HSI Segmentation) and 0.992 (using SegNet model) in the study of Dong et al. (2018). The discrepancy in accuracy can be attributed to human errors in the manual segmentation.

Segmentation results for the two images with the largest discrepancies in computed GVI values between model-derived and manually segmented outputs show some minor inaccuracies, including distortions along the upper and lower edges, and at stitching boundaries arising from image mosaicking, and subtle misclassifications on the ground surface and less dense tree canopies.

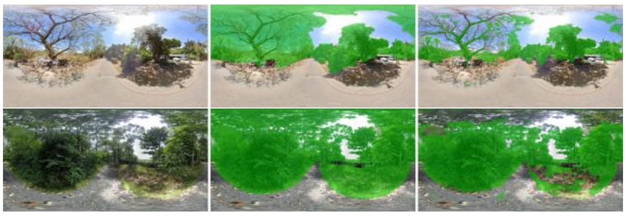

Figure 5. Sample segmentation results (left: original image, middle: manual segmentation, right: model segmentation)

However, a substantial portion of these discrepancies occur in images involving tall, dense, interconnected, and highly clustered vegetation, such that most of the greenery covers the top 360-degree view, which is uncommon in highly urbanized areas such as Metro Manila. In addition, occasional misclassifications, such as on the ground, are very small and can be considered negligible.

4.3 Visual Distribution and Descriptive Statistics of Urban Greenery (GVI) and Housing Price

The Green View Index (GVI) values range from 0 to 0.811 (mean = 0.101, SD = 0.099) and exhibit a positively skewed distribution, over 50% of points fall below 0.071 and 75% below 0.143, indicating that most streets in Metro Manila have low to medium visible greenery. This skew highlights spatial inequality in street-level greenery likely driven by differences in planning, socioeconomic status, and historic development, potentially leading to unequal access to green spaces and their associated benefits.

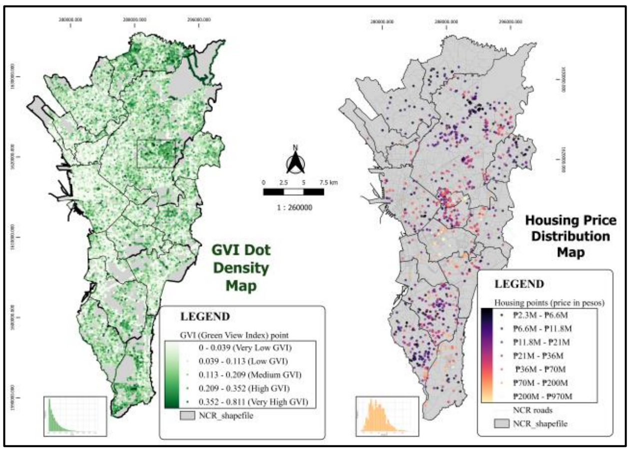

Figure 6. Visual Distributions of Greenery and Housing Price

In contrast, scraped house listings (single-family houses, townhouses, villas, and beach houses), show dense clustering in high-value, urbanized districts and sparse coverage elsewhere. Prices range from ₱2.3M to ₱970M (25th percentile = ₱9.5M), confirming right-skewness toward upper-end properties. As a result, model results predominantly reflect the high-end market rather than affordable housing.

Of the 1,007 listings in Figure 7, most are in Quezon City, followed by Parañaque and Las Piñas, confirming Lamudi's bias toward larger, more urbanized—and typically more expensive—areas. Five LGUs (Valenzuela, Pasay, Malabon, Pateros, Navotas) have less than 20 listings and were excluded from city-level analyses. Low representation in these LGUs likely reflects small land area (Pateros), specialized land uses (e.g., NAIA/Villamor in Pasay; large fish port in Navotas), higher flood risk and lower incomes (Malabon, Pateros, Navotas), or a stronger industrial/socialized-housing profile (Valenzuela).

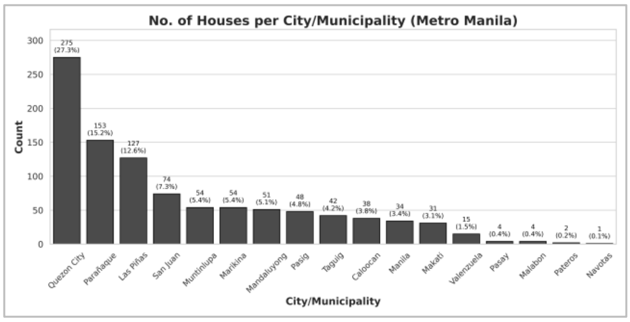

Figure 7. Distribution of House Listings per City/Municipality

The uneven distribution of housing points, with some areas having very few listings, reduces the representativeness of price aggregates in the cluster analysis and may undermine the reliability of city-level models.

4.4 Spatial Cluster and Hotspot Analysis

Getis–Ord Gi* and Anselin's Local Moran's I were applied to examine spatial clustering in GVI and housing prices. Gi* identifies statistically significant hotspots (clusters of high values) and coldspots (clusters of low values), while Local Moran's I detects local spatial autocorrelation, including High–High and Low–Low clusters and High–Low / Low–High outliers.

4.4.1 Urban Greenery Clusters: Getis–Ord Gi* shows an uneven GVI distribution with four primary hotspots: (1) La Mesa Watershed (northern Quezon City), (2) U.P. Diliman, (3) northeastern Marikina near the Upper Marikina River Basin, and (4) southern Muntinlupa. Much of the dense urban core and western Metro Manila (Manila, Pasay, Makati, Valenzuela, Navotas, Malabon, parts of Parañaque and Las Piñas) are cold spots.

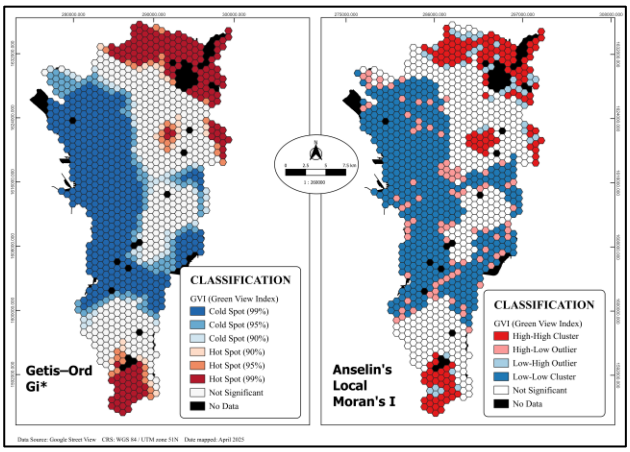

Figure 8. Hotspots and Clusters of Urban Greenery

Local Moran's I confirms these high–high clusters and identifies spatial outliers: high–low outliers (isolated green patches in low-GVI surroundings) such as at the Quezon City–San Juan border and Parañaque, and low–high outliers (unexpectedly low GVI within greener surroundings) often at the edges of clusters or along major infrastructure, notably the Muntinlupa–Cavite Expressway.

The results imply that, with the notable exception of U.P. Diliman, visible-greenery hotspots in Metro Manila are predominantly peripheral (north, northeast, south) where natural or institutional green spaces remain intact, whereas minimal visible greenery concentrates in the dense core, around the middle and western built-up areas.

This spatial heterogeneity has important consequences for greenery–price relationships. In hotspot areas, abundant greenery may produce diminishing marginal effects on housing prices. Conversely, in coldspot regions—where greenery is scarce—even modest visible-greenery gains may command a premium because they are rare amenities.

High–high clusters suggest regions where consistent greenery may stabilize or elevate property values across a broad area; low–low clusters indicate zones where limited greenery may uniformly depress prices. Spatial outliers (high–low and low–high) highlight local contrasts that can amplify or suppress these trends at finer scales. This significant clustering of GVI is reflected in its Global Moran's I = 0.723 (p = 0.001), indicating strong spatial autocorrelation and necessitating spatial lag/error specifications or cluster-robust inference in the hedonic price models to avoid biased estimates.

The spatial pattern of greenery aligns with observations from other rapidly urbanizing cities. In Jakarta, many unmanaged and larger urban green spaces are scattered in the city's outskirts, while smaller fragments dot the inner districts, which also host the highest population densities (Hwang et al., 2020).

4.4.2 Housing Price Clusters: Getis–Ord Gi* shows major housing-price hotspots in the center of Metro Manila—around central business districts in San Juan, Mandaluyong, Makati, Pasig, and Taguig—and a southern cluster near Muntinlupa (Filinvest City). Coldspots occur in the northern periphery (Valenzuela, North Caloocan, Quezon City) and parts of Marikina and Las Piñas. Since the dataset includes only 1007 house listings and is not well distributed, many areas of Metro Manila are not covered.

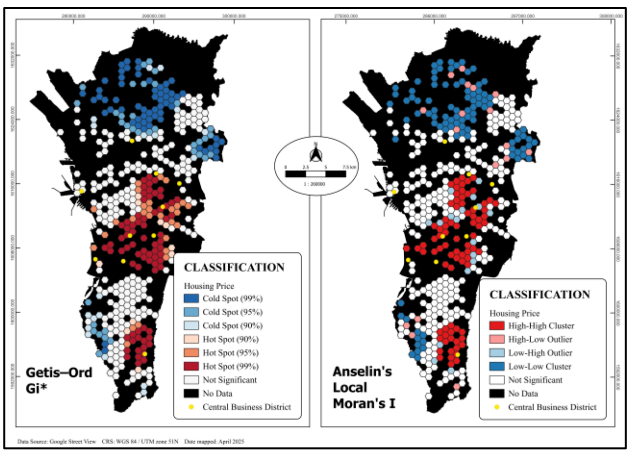

Figure 9. Hotspots and Clusters of Housing Prices

Local Moran's I confirms the High–High and Low–Low clusters and also identifies High–Low and Low–High outliers along cluster edges — areas having early gentrification (luxury units in lower-priced neighborhoods) or undervalued properties within expensive districts.

These spatial patterns are largely explained by urban centrality: proximity to CBDs increases access to jobs, services, commercial activities, and infrastructure and therefore tends to raise prices. In contrast, peripheral areas especially in the northern parts, are farther from these economic hubs and generally show lower prices. However, outliers indicate that localized factors—such as luxury developments in otherwise low-price areas (High-Low) or depressed prices near CBDs due to issues like poor infrastructure or high crime rates (Low-High) —can override and deviate from this general trend at finer scales. The significant clustering of housing prices is also reflected in its Global Moran's I = 0.577 (p = 0.001), indicating a fairly strong spatial autocorrelation, which further necessitates spatial lag/error specifications or cluster-robust inference in subsequent hedonic models.

Comparing the GVI and housing-price maps reveals spatial divergence: high GVI clusters are mostly peripheral (north and south edges), while high price clusters are mostly central. This spatial disconnect suggests that greenery and housing prices follow distinct patterns. Greenery thrives in outer regions, bordering less urbanized provinces, while expensive houses cluster near central business districts. This does not imply a simple negative causal effect of GVI on prices: rather, it highlights that other factors, such as proximity to business districts, infrastructure, or accessibility, may be greater influencers of housing prices. To understand the marginal impact of GVI on housing price, while controlling for confounding variables, hedonic price modelling is necessary.

4.5 Hedonic Price Modelling

Hedonic models are estimated at three scales: overall Metro Manila, by Local Climate Zone (LCZ), and by city to compare GVI's effect across different urban environments and test for consistent patterns. Pairwise correlations among sub-variables are all < |0.70| and all variance inflation factors (VIFs) are < 5 for the overall model, indicating no problematic multicollinearity.

4.5.1 Overall Model: The overall model in Table 1 reveals that the Green View Index (GVI) is positively and significantly associated with housing prices ($\beta = 0.107$, $p < 0.001$). A one standard deviation increase in GVI raises the natural logarithm of housing price by 0.107. Practically, this is equivalent to a 2.65% increase in price for every 0.01 rise in average GVI within a 400-meter radius. 805 observations were used for training, while 202 were allocated for testing. The training R^2 and testing R^2 are 0.495 and 0.547, respectively.

Variable	Coefficient	[95% CI Lower, Upper]	p-value
Location	0.094	[0.019, 0.169]	0.014
Structural/Housing	0.972	[0.898, 1.046]	0.000
Proximity	-0.02	[-0.150, 0.110]	0.763
Density	0.144	[0.034, 0.253]	0.010
GVI	0.107	[0.057, 0.158]	0.000
No. Observations	805		
F-statistic	156.6	p = 6.24e-116	
R^2	0.495		
Adj. R^2	0.492		
Testing R^2	0.547		
Testing MSE	0.446		

Table 1. Linear Regression Results for Overall Model

Of the five predictors, four have positive and significant coefficients; the structural/housing predictor has the largest coefficient (0.972), confirming its dominant role in price determination (Biljecki and Ito, 2021). GVI ranks third in coefficient magnitude, but ranks second in statistical significance, highlighting its relatively consistent effect. Proximity (a composite of distances to amenities) shows a negative but insignificant effect, likely reflecting mixed effects of different amenities (some increase desirability, others introduce noise or disamenities). While not the primary driver, GVI exerts a meaningful impact that merits consideration in urban planning and housing market analyses.

4.5.2 LCZ-Based Models: LCZ-based models were constructed to assess how GVI's price effect varies by urban form. The regression models in Table 2 reveal that, while structural and housing attributes remain the dominant drivers of housing prices across Metro Manila, urban greenery exerts a consistent and meaningful premium, with effects that vary by urban form. LCZ 4 was omitted due to insufficient data.

LCZ Model	Variable Coefficient				
	Location	*Structural/ Housing*	*Proximity*	*Density*	*GVI*
Overall	0.094^{*}	0.972^{***}	-0.020	0.144^{*}	0.107^{***}
1	-0.038	1.265^{***}	0.790^{**}	-0.307	-0.051
2	0.165	0.975^{***}	0.004	-0.037	0.110
3	0.101^{*}	0.910^{***}	-0.043	0.130	0.064
5	0.697^{**}	1.102^{***}	0.316	-0.307	0.302^{*}
6	0.044	1.087^{***}	-0.110	0.304^{*}	0.150^{**}
7	0.133	0.558^{**}	0.172	-0.255	0.199
8	0.170	1.078^{***}	-0.111	0.380	0.217
9	0.645	1.101^{***}	-0.487	-0.105	0.209

Note: *p<0.05; **p<0.01; ***p<0.001

Table 2. Coefficients Across LCZ-Based Models

The key variable, GVI, significantly influences housing prices in LCZs 5 (Open Mid-Rise, β=0.302, p<0.05) and 6 (Open Low-Rise, β=0.150, p<0.01), where lower density and greater visibility enhances greenery's value.

In contrast, GVI has a negative but insignificant effect in LCZ 1 (Compact High-Rise, β=-0.051), possibly due to limited greenery presence and diluted effects. In other LCZs (2, 3, 7, 8, 9), GVI remains insignificant, though some LCZs (3, 8, and 9) have p-values near 0.10, hinting at marginal effects. A more detailed analysis is as follows:

4.5.2.1. Compact Group (LCZ 1-3): The Compact group which includes LCZ 1 (Compact High-Rise), LCZ 2 (Compact Mid-Rise), and LCZ 3 (Compact Low-Rise), is characterized by dense arrangements of buildings with limited greenery. In these zones, structural and housing attributes dominate price determination. GVI's effect is minimal and statistically insignificant overall, though LCZ 3 shows a weak positive trend (p = 0.105), plausibly because lower building heights increase the visibility and appreciation of street greenery. The uniform scarcity of greenery likely reduces its perceived value, as additional trees do not substantially alter the urban landscape or resident priorities. In addition, the highly congested environment likely dilutes any perceived positive effects of greenery in this urban form. Other competing priorities in housing decisions further reduce greenery's perceived value.

4.5.2.2. Open Group (LCZ 5-6):
The Open group comprises LCZ 5 (Open Mid-Rise) and LCZ 6 (Open Low-Rise), featuring open arrangements of buildings with abundant pervious land cover. Here, GVI has the strongest and most consistent positive association with housing prices: LCZ 5 (β = 0.302, p < 0.05) and LCZ 6 (β = 0.150, p < 0.01). The lower density and greater visibility of greenery make it a valued amenity, particularly in LCZ 5, where urban-suburban transitions and greater access to employment amplify its impact. In LCZ 6, consistent greenery visibility due to lower building heights ensures its contribution to property values and higher significance. Quantitatively, a 0.01 increase in GVI within a 400-meter radius corresponds to an estimated price increase of 7.65% in LCZ 5 and 3.72% in LCZ 6.

4.5.2.3. Mixed Group (LCZ 7-9):
The Mixed group, which includes LCZ 7 (Lightweight Low-Rise), LCZ 8 (Large Low-Rise), and LCZ 9 (Sparsely Built), encompasses a heterogeneous mix of urban forms, from dense informal settlements to sparsely built natural settings. GVI is not a significant predictor of prices in these zones. The absence of a clear green premium may reflect low within-zone variability in greenery (either uniformly scarce in LCZs 7–8 or uniformly abundant in LCZ 9) or opposing local land-use effects depending on the prevailing building typology (e.g., warehouses, factories, cemeteries vs. retail stores, golf courses, or campuses). Other considerations such as affordability in LCZ 7 appear to outweigh street-level greenery in buyer preferences.

Overall, greenery's effect is strongest and most robust in the Open zones (LCZ 5 and 6), where lower density and improved visibility magnify its value. In Compact (LCZ 1–3) and Mixed (LCZ 7–9) zones the effect is negligible, likely due to built-form dominance, differing resident priorities, or mixed local land-use impacts.

4.5.3 City-Based Models
To assess local heterogeneity, hedonic models were constructed separately for each city, where density, land area, and socioeconomic conditions differ. Results in Table 3 show that GVI's effect on prices is spatially variable and significant only in a few cities.

City	Ave GVI	GVI coeff	R^2	Test R^2	MSE
Makati	0.09	0.57^{**}	0.62	0.34	1.03
Manila	0.06	0.48^{**}	0.61	0.82	0.05
Mandaluyong	0.08	0.26	0.36	0.20	0.88
Las Piñas	0.11	0.18	0.63	0.51	0.37
Pasig	0.10	0.17	0.58	0.02	0.77
Taguig	0.08	0.06	0.70	0.53	0.48
Muntinlupa	0.14	0.05	0.56	0.45	0.32
Parañaque	0.09	0.04	0.57	0.36	0.23
Marikina	0.10	0.01	0.46	-0.42	0.45
Quezon City	0.12	-0.01	0.63	0.16	0.43
San Juan	0.08	-0.04	0.43	-1.49	1.37
Caloocan	0.12	-0.09	0.58	-0.56	0.34

Note: *p<0.05; **p<0.01; ***p<0.001

Table 3. Coefficients Across City-Based Models

GVI is a positive and statistically significant predictor of housing prices in Makati (β = 0.57, p = 0.003) and Manila (β = 0.48, p = 0.008); it is marginal in Las Piñas (β = 0.18, p = 0.065) and not significant elsewhere. Cities with the largest absolute GVI coefficients (Makati, Manila, Mandaluyong, Las Piñas, Parañaque) also tend to have lower p-values, suggesting a generally positive relationship between greenery and housing prices, even if not all coefficients achieve conventional significance ($p < 0.05$). Quezon City, San Juan and Caloocan show small negative GVI coefficients ($p = 0.69$, 0.873 and 0.51, respectively), indicating context-specific factors or data limits.

Model fit and predictive accuracy vary across cities: training R^2 ranges from 0.36 (Mandaluyong) to 0.70 (Taguig). Testing MSEs also diverge (best in Manila, MSE = 0.05; worse in Makati, MSE = 1.0336), suggesting differing model reliability and market complexity. Makati's higher MSE (1.0336), despite a significant positive GVI coefficient, points to a more complex housing market where factors like prestige, developer reputation, or luxury amenities may play a larger role. This is reinforced by the fact that Makati is the only city where the Structural/Housing composite is not a significant predictor, unlike all others where it is highly significant ($p < 0.01$).

Explanations for the spatial pattern are consistent with centrality and urban form. GVI's prominence in Makati and Manila likely stems from their dense urban form, where scarce green space is highly valued. In Makati, the financial hub, the large GVI coefficient (0.572) highlights the premium on greenery as a prestige factor within a high-end market. In Manila, the historical capital, the significant coefficient (0.475) reflects a consistent valuation of greenery amid dense development and limited open space.

However, cities with high average GVI (Muntinlupa, Quezon City, Caloocan) but weak or negative GVI effects show that abundant greenery alone does not guarantee a price premium. Spatial heterogeneity helps explain this: Quezon City's large, mixed urban fabric dilutes uniform GVI effects; San Juan's small area results in limited within-city GVI variation yielding noisy estimates; and Caloocan's fragmented development produces overgrown vacant lots associated with lower-price neighborhoods (especially in North Caloocan).

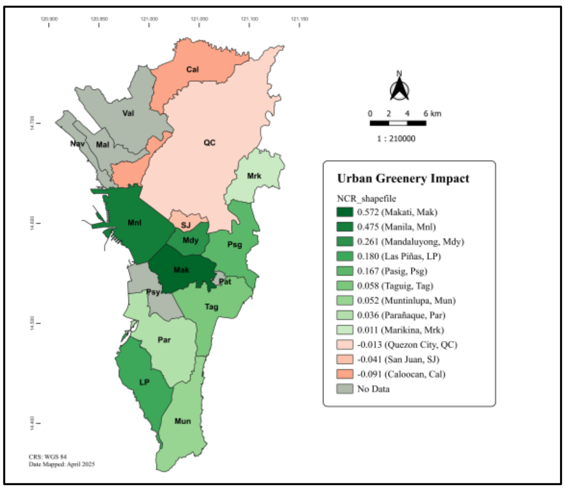

Figure 10. Urban Greenery Impact Across the Different Cities

Central cities (Manila, Makati, Mandaluyong, Pasig) exhibit the strongest positive GVI coefficients. Positive but weaker effects extend southward to Taguig, Parañaque, Las Piñas and Muntinlupa, producing a southward gradient of GVI impact. By contrast, northern-periphery cities (Caloocan, Quezon City, San Juan) show lower or negative coefficients indicating a relatively lesser or negligible impact of greenery on housing prices. Northwestern cities (Navotas, Malabon, Valenzuela) have insufficient observations, likely due to Lamudi's bias toward upper-end listings, which limits their representation. Overall, the results imply that the economic value of visible greenery is spatially varying and supports context-specific urban planning to maximize the economic benefits of greenery across Metro Manila's diverse cities.

5. Conclusion and Recommendations

5.1 Conclusion

This study examined the relationship between street-level greenery and housing prices across urban local climate zones (LCZs) in Metro Manila. Greenery was quantified via the Green View Index (GVI) from Google Street View panoramas sampled at 100-m intervals, averaged within a 400-m radius of housing units scraped from Lamudi, and integrated into hedonic pricing models alongside traditional housing factors at the whole Metro Manila area, LCZ-specific, and city-specific scales.

Results confirm that structural factors remain the primary determinants of property values, but visible greenery yields a positive premium in open urban forms. In LCZ 5 (Open Mid-Rise), a 0.01-unit GVI increase raises housing prices by 7.65% ($\beta = 0.302$, $p = 0.020$); in LCZ 6 (Open Low-Rise), by 3.72% ($\beta = 0.150$, $p = 0.003$), reflecting how open areas enhance visibility and appreciation of greenery. By contrast, in denser, compact zones (LCZ 1–3 and LCZ 7), and in the large low-rise or sparsely built areas (LCZ 8 and LCZ 9), greenery effects are statistically insignificant – likely because greenery is limited, unprioritized, less visible, and has low variability.

City-level analysis showed strongest GVI impacts in central, dense cities like Makati ($\beta = 0.57$, $p = 0.003$) and Manila ($\beta = 0.48$, $p = 0.008$), where greenery is a scarce amenity. Conversely, in cities with more abundant or unmanaged greenery, such as Quezon City and Caloocan, the effect of GVI is negligible or even negative. In these areas, factors like informal settlements, flood-prone zones, or overgrown vacant lots may reduce the perceived value of greenery, particularly in northern peripheral areas like North Caloocan.

Integrating the LCZ-based and city-based findings reveals that the value of urban greenery is highly context-dependent. This suggests that the quality, visibility, and integration of greenery within specific urban configurations—rather than its mere presence—drive its economic value.

5.2 Recommendations

Future research should more closely align image-capture dates with housing transaction timestamps, expand sample sizes for under-represented LCZs and cities, and apply preprocessing measures to reduce image distortions. To improve generalizability to middle- and low-income segments, use representative datasets spanning all price levels—sourcing from multiple platforms or stratified sampling to reduce bias toward upscale properties like those on Lamudi. Enhance model robustness by testing for heteroskedasticity (via robust White standard errors), adding spatial lag terms, addressing potential endogeneity, and considering AIC (Akaike Information Criterion) as a metric in comparing the models. Incorporate additional variables for greater explanatory power, such as flood risk, to assess their distinct price impacts, enabling more accurate predictions.

https://doi.org/10.5194/isprs-archives-XLVIII-5-W4-2025-159-2026

References

An, S., Jang, H., Kim, H., Song, Y., Ahn, K., 2023: Assessment of street-level greenness and its association with housing prices in a metropolitan area. Scientific Reports, 13(1). doi.org/10.1038/s41598-023-49845-0.

Android Police, 2023: How often does Google Maps update Street View? https://www.androidpolice.com/how-often-google-maps-updates-street-view/ (25 August 2023).

Biljecki, F., Ito, K., 2021: Street view imagery in urban analytics and GIS: A review. Landscape and Urban Planning, 215, 104217. doi.org/10.1016/j.landurbplan.2021.104217.

Chen, J., Zhou, C., Li, F., 2020: Quantifying the green view indicator for assessing urban greening quality: An analysis based on Internet-crawling street view data. Ecological Indicators, 113, 106192. doi.org/10.1016/j.ecolind.2020.106192.

CSAILVision, n.d.: semantic-segmentation-pytorch [Computer software]. GitHub. https://github.com/CSAILVision/semantic-segmentation-pytorch (accessed 24 May 2024).

Dimoudi, A., Nikolopoulou, M., 2003: Vegetation in the urban environment: microclimatic analysis and benefits. Energy and Buildings, 35(1), 69–76. doi.org/10.1016/s0378-7788(02)00081-6.

Dong, R., Zhang, Y., Zhao, J., 2018: How green are the streets within the Sixth Ring Road of Beijing? An analysis based on Tencent Street View Pictures and the Green View Index. International Journal of Environmental Research and Public Health, 15(7), 1367. doi.org/10.3390/ijerph15071367.

Hwang, Y. H., Nasution, I.K., Amonkar, D., Hahs, A., 2020: Urban green space distribution related to land values in Fast-Growing megacities, Mumbai and Jakarta – Unexploited opportunities to increase access to greenery for the poor. Sustainability, 12(12), 4982. doi.org/10.3390/su12124982.

Lamudi Philippines, 2024–2025: Lamudi property listings [Data set]. Lamudi. https://www.lamudi.com.ph (retrieved 25 May 2024; 25 January 2025; 2 March 2025).

Li, X., Zhang, C., Li, W., Ricard, R., Meng, Q., Zhang, W., 2015: Assessing street-level urban greenery using Google Street View and a modified green view index. Urban Forestry & Urban Greening, 14(3), 675–685. doi.org/10.1016/j.ufug.2015.06.006.

OpenStreetMap contributors, n.d.: OpenStreetMap [Data set]. OpenStreetMap. https://www.openstreetmap.org (accessed 12 June 2024).

Qian, Y., Zhou, W., Yu, W., Pickett, S. T. A., 2015: Quantifying spatiotemporal pattern of urban greenspace: new insights from high resolution data. Landscape Ecology, 30(7), 1165–1173. doi.org/10.1007/s10980-015-0195-3.

Ramos, R., Tamondong, A., Torres, R. A., Recto, B. A., Panlilio, K., Ana, R. R. S., Tinio, M. L., Yumul-Calzado, T., Carcellar, B., III, Cayetano, M., 2024: Enhancing Government Capacity for Air Quality Management in the Philippines through Geospatial Technologies: A Case of Project AiRMoVE. ISPRS Annals of the Photogrammetry, Remote Sensing and Spatial Information Sciences, X-5–2024, 151–158. doi.org/10.5194/isprs-annals-x-5-2024-151-2024.

Stewart, I. D., Oke, T. R., 2012: Local climate zones for urban temperature studies. Bulletin of the American Meteorological Society, 93(12), 1879–1900. doi.org/10.1175/bams-d-11-00019.1.

Stubbings, P., Peskett, J., Rowe, F., Arribas-Bel, D., 2019: A hierarchical urban forest index using Street-Level imagery and deep learning. Remote Sensing, 11(12), 1395. doi.org/10.3390/rs11121395.

Wittowsky, D., Hoekveld, J., Welsch, J., Steier, M., 2020: Residential housing prices: impact of housing characteristics, accessibility and neighbouring apartments – a case study of Dortmund, Germany. Urban, Planning and Transport Research, 8(1), 44–70. doi.org/10.1080/21650020.2019.1704429.

Wu, D., Gong, J., Liang, J., Sun, J., Zhang, G., 2020: Analyzing the influence of urban street greening and street buildings on summertime air pollution based on Street View image data. ISPRS International Journal of Geo-information, 9(9), 500. doi.org/10.3390/ijgi9090500.

Yang, J., Zhao, L., McBride, J. R., Gong, P., 2009: Can you see green? Assessing the visibility of urban forests in cities. Landscape and Urban Planning, 91(2), 97–104. doi.org/10.1016/j.landurbplan.2008.12.004.

Zhang, Y., Dong, R., 2018: Impacts of Street-Visible Greenery on Housing Prices: Evidence from a Hedonic Price Model and a Massive Street View Image Dataset in Beijing. ISPRS International Journal of Geo-information, 7(3), 104. doi.org/10.3390/ijgi7030104.

Zhao, H., Shi, J., Qi, X., Wang, X., Jia, J., 2017: Pyramid Scene Parsing network. https://openaccess.thecvf.com/content_cvpr_2017/html/Zhao_Pyramid_Scene_Parsing_CVPR_2017_paper.html (accessed 24 May 2024).

Zhou, B., Zhao, H., Puig, X., Fidler, S., Barriuso, A., Torralba, A., 2017: Scene parsing through ADE20K dataset. 2017 IEEE Conference on Computer Vision and Pattern Recognition (CVPR), 5122–5130. doi.org/10.1109/CVPR.2017.544.